

## Gold-Bearing Arsenide and Other Production-Well Scales from the Salton Sea Geothermal Field, California

Susan Juch Lutz<sup>1</sup>, Jeffrey B. Hulen<sup>1</sup>, and William L. Osborn<sup>2</sup>

<sup>1</sup>Energy & Geoscience Institute, University of Utah  
423 Wakara Way, Suite 300, Salt Lake City, UT 84108  
sjlutz@egi.utah.edu, jhulen@egi.utah.edu

<sup>2</sup>CalEnergy Operating Corporation.  
950 West Lindsey Road, Calipatria, CA 92233  
will.osborn@calenergy.com

### ABSTRACT

Hot (up to 365°C), metalliferous brines of different concentrations in the Salton Sea geothermal system yield production-well scales with correspondingly varied mineralogy and texture also reflecting the composition of the casing material. Titanium liners in the upper parts of some wells accumulate mostly amorphous iron silicate (probably hisingerite) and poorly-crystalline, iron-rich nontronite, along with minor magnetite, sphalerite, and chalcopyrite. Deeper scales deposited near flashpoints on cement-lined steel casing consist mostly of bismuth-, copper-, and locally gold-rich loellingite (FeAs<sub>2</sub>). One such scale sample from the northern part of the field is almost all coarsely crystalline loellingite with a crudely bladed habit. Although from a deposit at most a few kg in weight, the arsenide in this scale boasts bonanza gold grades of up to 233 grams (8.2 oz) per ton.

Scales precipitated from relatively less saline (about 23 wt % total dissolved solids; TDS) brines in the southwestern part of the Salton Sea system are dominated by iron-rich nontronite with scattered magnetite microlaminae. Dehydration cracks and local botryoidal banding of the clay could indicate either direct precipitation from a gel-like state, or alteration of initial hisingerite already crystallized from such a gel. More concentrated (about 30 wt % TDS) brines in the northern part of the system typically deposit layered scales with alternating bands of hisingerite, nontronite, and loellingite. Soft, iron-rich scales dominated by nontronite are much more amenable to periodic wellbore cleanout than are glassier and harder varieties consisting mostly of hisingerite. The precise combination of variables favoring formation of the preferred layer silicate remain to be fully determined.

### INTRODUCTION

The metal-rich brines of the Salton Sea geothermal system have received much attention from the international scientific community. The Salton Sea geothermal system is considered one of the largest (> 1,000 MW possible) and hottest (up to about 350°C) water-dominated fields in the world. However, the brine is characterized as an extremely high salinity liquid with the concentration of total dissolved solids greater than 200,000 ppm. The combination of the chemistry and the high temperature of the Salton Sea brine has led to the principal challenges in both the development of the geothermal resource and the metal recovery process: scaling and corrosion of production wells, piping, steam-gathering and surficial plant equipment, and injection wells.

The large throughput of fluids associated with the production of electricity (a total of 330 MWe) allows for the low-cost recovery of zinc from the brine which has about 500 ppm Zn (McKibben and Hardie, 1997). CalEnergy's Zinc Recovery Project is expected to produce an estimated 30,000 metric tons of zinc per year, with the associated facilities producing 49 megawatts (net) of geothermal electricity (GRC Bulletin, Sept/Oct 1999). Yet even as CalEnergy prepares to produce its first ingot of zinc from the Salton Sea brine, scaling continues to be a problem. Older carbon steel-cased wells are being replaced with new corrosion-resistant titanium casing, and the amount of scaling in the production wells has been dramatically reduced, but not eliminated.

The purpose of this study is to characterize the mineralogy and chemistry of selected production well scales from the Salton Sea geothermal field.

The overall objective is to compare the scale chemistry to the fluid chemistry in several production areas, and to relate the type of scale deposited on different casing materials in the wells under a variety of borehole conditions or processes (such as boiling). This is a cooperative project between EGI and CalEnergy Operating Corp., and is part of a larger DOE-funded study on the geology of the Salton Sea geothermal system. Petrographic, X-ray diffraction, elemental chemistry, scanning electron microscope, and electron microprobe techniques were used to characterize scale samples from four production wells. These four samples represent two major producing areas of the Salton Sea geothermal field, and two types of production wells, three wells with titanium casing and one with a cement-lined carbon steel liner.

### **TEXTURAL, MINERALOGICAL AND CHEMICAL DESCRIPTION OF PRODUCTION WELL SCALES**

The scales samples are from four production wells, Sinclair 10 and 11 (SI-10 and SI-11) located in Region I producing area to the southwest, and Elmore 12 (EL-12) and River Ranch 18 (RR-18) located in Region III, in the northeastern part of the field (Fig. 1). All of the brines produced in the Salton Sea field have temperatures between 300° and 350 °C, and are near neutral with a pH of 5.5, and an Eh of about 220 mV. Production fluids in the southern part of the geothermal field are less saline (with 23 wt % TDS) than fluids to the north (with up to 30 wt % TDS). The major and minor element chemistry of the scales from the three titanium-cased wells (SI-10, SI-11 and EL-12) may reflect this trend in the fluid chemistry (see Table 1). There is a general increase in alkali (Na, K, Mg), precious (Au), and other metals (As, Co and Ni); and a decrease in base (Cu, Pb, Zn) and other metals (Fe, Mn, Ca, P, Ba and V) in the scale chemistry from the Sinclair wells northward to the Elmore well.

#### **Scale from Wells Sinclair 10 and Sinclair 11**

The Sinclair scales were recovered during 1999 after the original steel-cased wells had been replaced with non-corrosive titanium casings. The two wells are closely spaced and produce fluids with about 23 wt % TDS. The scales are similar in texture and mineralogy, composed predominantly of translucent orange-brown to red-brown, fibrous to botryoidal, poorly crystalline clay. Some patches of fibrous, olive-green clay are present within the orange-brown fibrous material. Healed dehydration cracks suggest that the scale material was initially a gel and that the clay crystallized from an originally amorphous iron silicate phase, likely similar to hisingerite [Fe(OH)<sub>3</sub>\*SiO<sub>2</sub>; Gallup, 1989, 1993; Gallup and Reiff, 1991]. The SI-11 scale sample contains minor opaque

material (1 to 2 wt % magnetite based on X-ray diffraction analyses), iron oxides that cement clasts of the orange-brown scale, and traces of calcite and quartz.

An X-ray diffraction (XRD) pattern of the clay in the scale indicates that it is a very poorly crystalline smectite (001 peak at 14-15Å and 060 peak at 1.53 Å). Based on its color, it is likely that this iron-rich smectite is similar to nontronite (see below). In thin section, the fibrous material is all, more or less, birefringent indicating that no truly amorphous material is present.

A thin crust of light-colored, botryoidal material in the SI-10 scale sample was analyzed by electron microprobe. Backscattered electron images and element distribution maps (Fig. 2) demonstrate that this material is composed of Ca-, Fe- and Mn-rich carbonate which was deposited on underlying botryoidal iron silicate material. Darker bands in the carbonate contain Zn, Fe and S (see figures 2c-d) suggesting the presence of thin layers of Fe-bearing sphalerite in the scale.

#### **Scale from Well Elmore-12**

Production well Elmore-12 (EL-12) is cased with titanium alloy, and the scale was collected from the well during 1999. The brine produced from this well has about 28 wt % TDS. The scale sample consists of fragments of dark brownish gray to slightly greenish-colored material. Petrographically, the scale exhibits two textural varieties; one is dense and botryoidal to fibrous with thin bands of an opaque metallic mineral, and the other is cellular and spherulitic. Desiccation cracks in both types of material indicate that it crystallized from a gel-like state.

X-ray diffraction analyses indicate that the scale is composed of poorly crystalline smectite similar to that observed in the Sinclair wells, and X-ray amorphous iron silicate glass. The disseminated metallic phase is loellingite (FeAs<sub>2</sub>). Traces of quartz, anhydrite, and halite are also present. Backscattered electron images and element mapping from the electron microscope (Fig. 3a-d) illustrate the fibrous texture and composition of the smectite. SEM images, shown in Fig. 3e, illustrate the conchoidal fracturing and glassy character of the amorphous iron silicate. EDX spectra of the glass show the dominant elemental peaks for Si, O, and Fe (Fig. 3f). In places the dense Fe-silicate glass is coated with pure Si opal spherules.

Whole-rock chemistry (Table 1) and electron microprobe analyses (Table 2) indicate the composition of the smectitic clay. Using the methodology of Moore and Reynolds (1989) and the

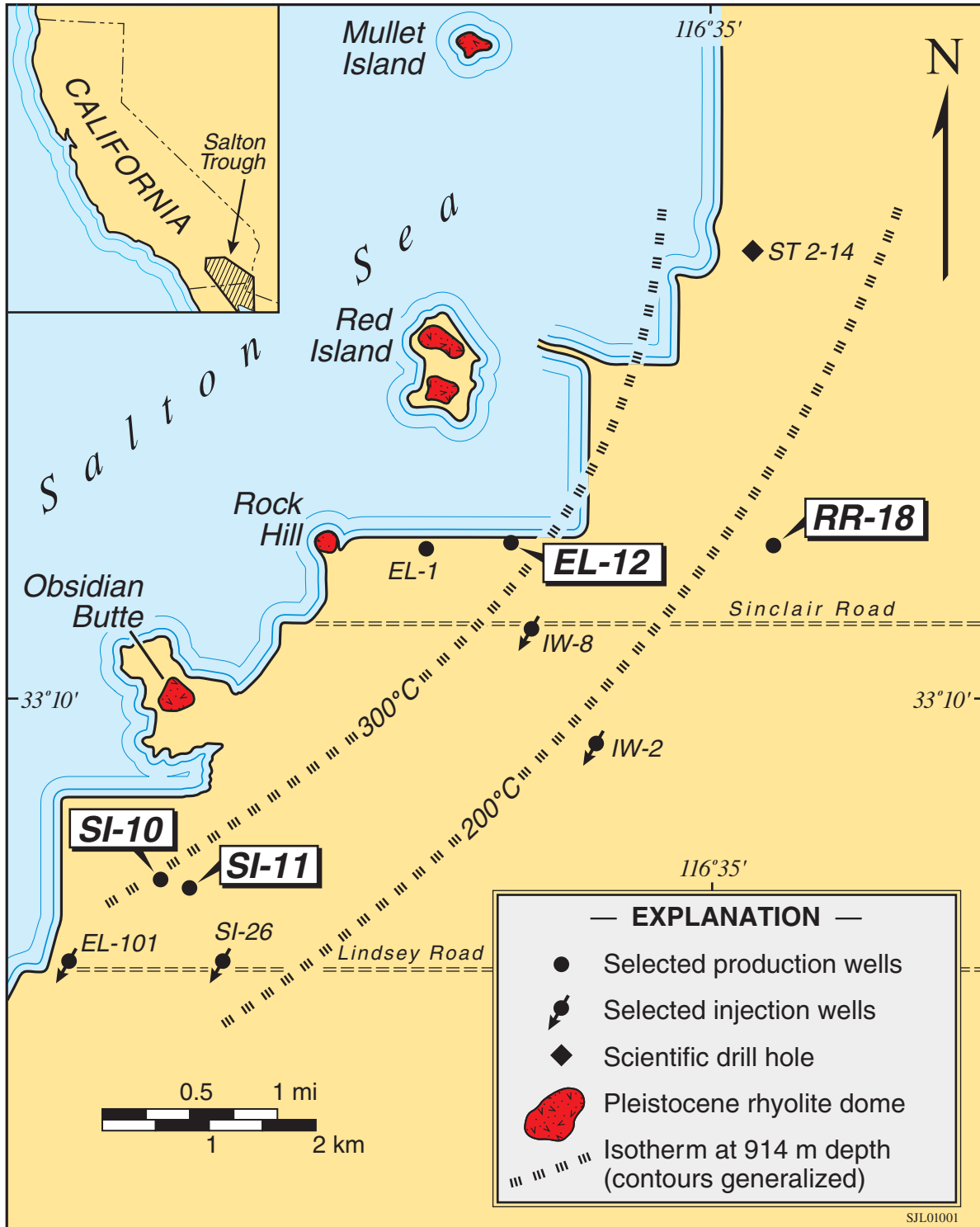
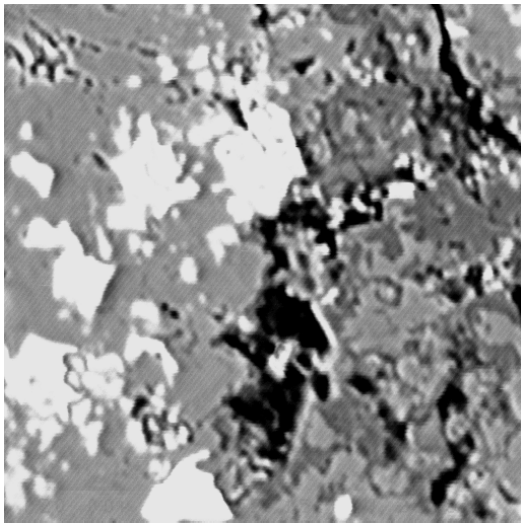
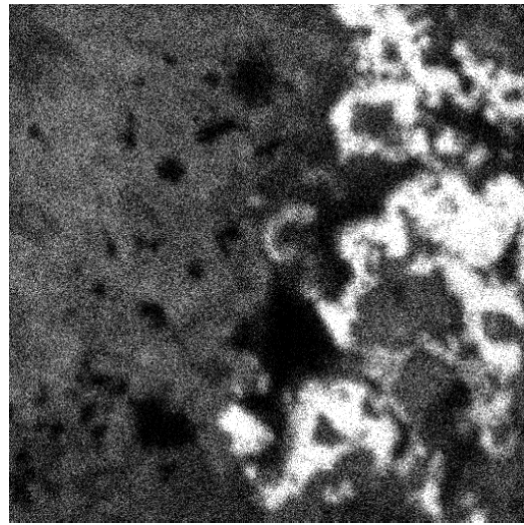


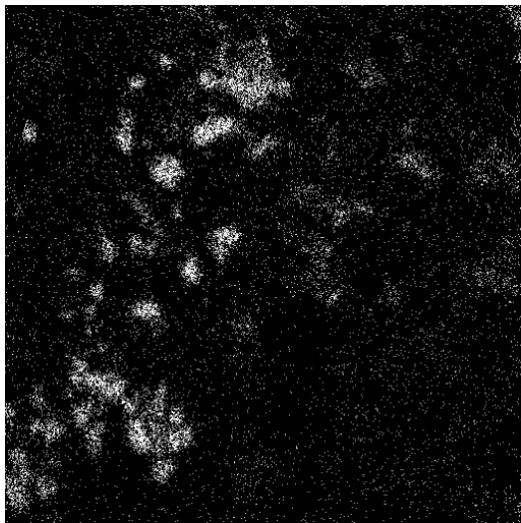
Figure 1. Map of the Salton Sea geothermal field within the Salton Trough in California. Quaternary rhyolite flow/dome locations and isotherms at 914 m depth modified from Elders and Sass (1988). Salton Sea shoreline from a 1989 Unocal Corporation photomosaic. Abbreviations as follows: EL = Elmore; IW = injection well; SI = Sinclair; ST = State; RR = River Ranch.



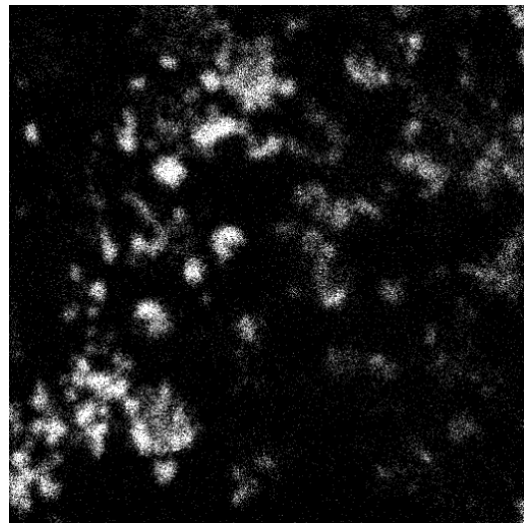
a. ABS



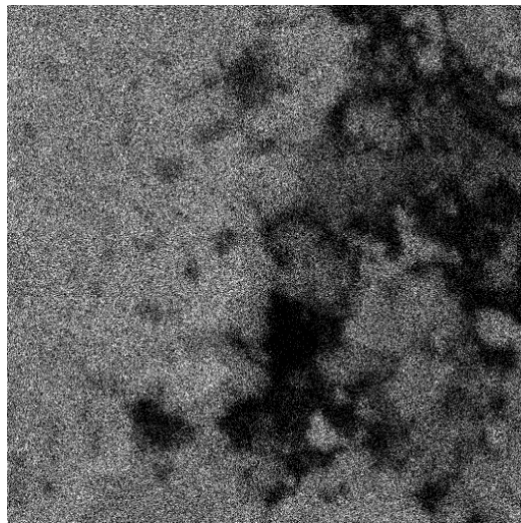
b. Ca



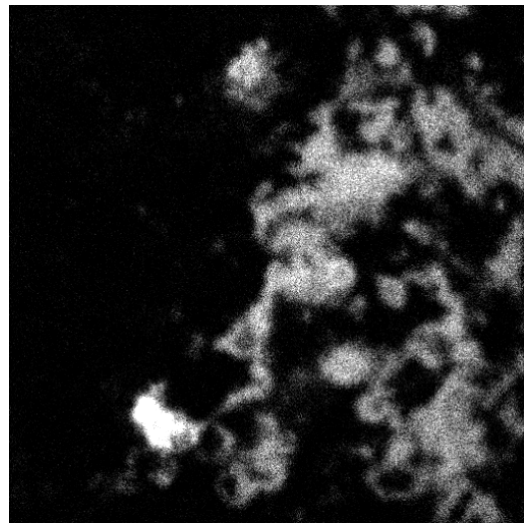
c. Zn



d. S



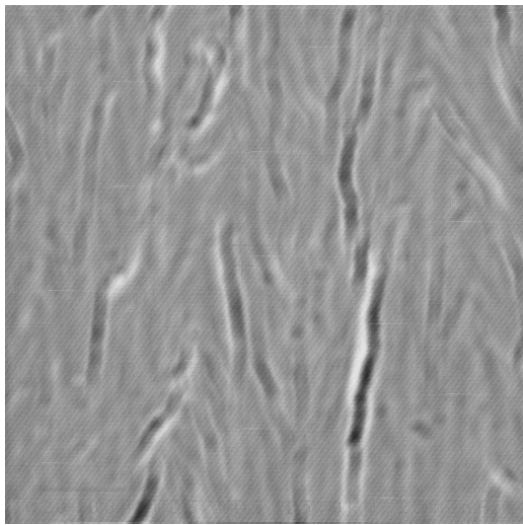
e. Fe



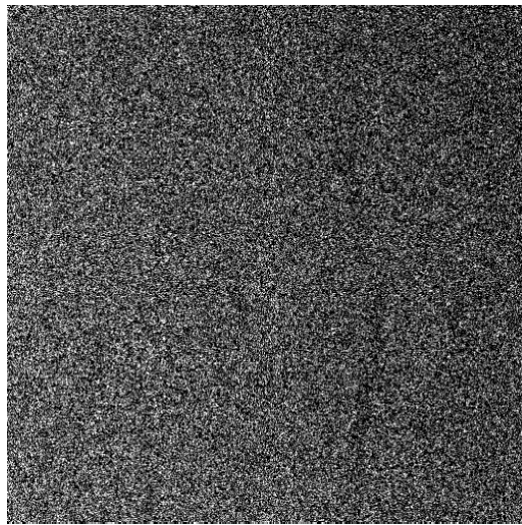
f. Si

SIL01002

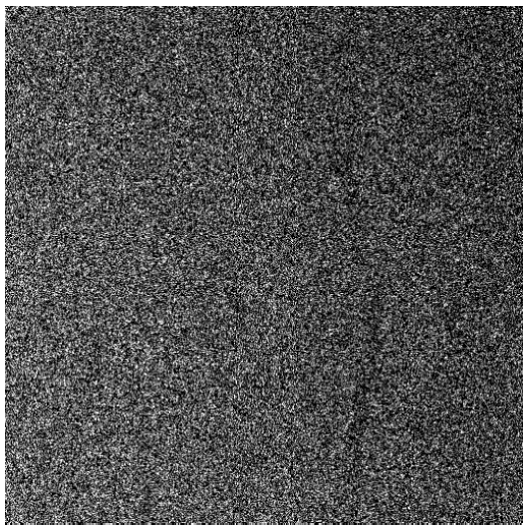
*Figure 2. Electron microprobe imagery and element mapping of scale from the Sinclair-10 well. Backscattered electron image of a portion of the scale showing botryoidal and crustiform texture of banded Ca-, Fe-, and Mn-carbonate, Fe-bearing sphalerite (ZnS), and Fe-silicate material (Fig. 2a; ABS = absorbed image). Scans for selected elements in the area depicted in 2a are shown in Figures 2b-e.*



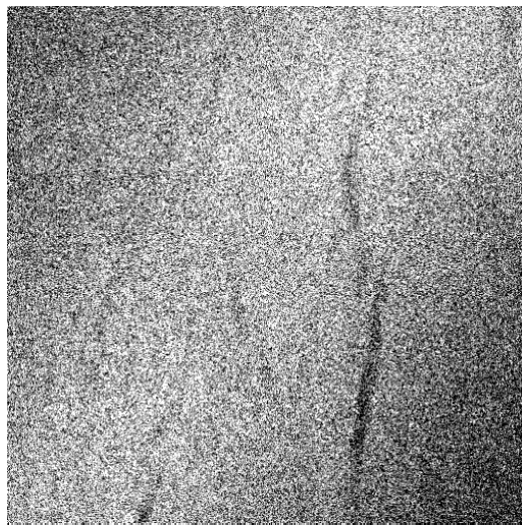
a. ABS



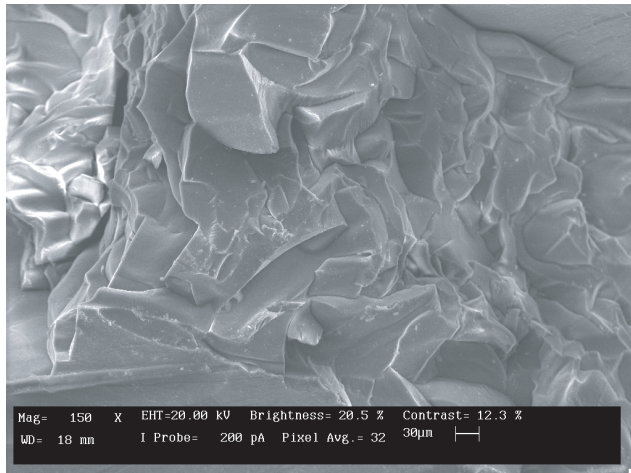
b. Mg



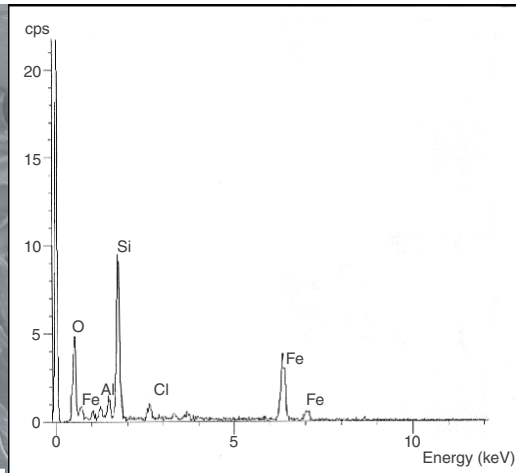
c. Fe



d. Si



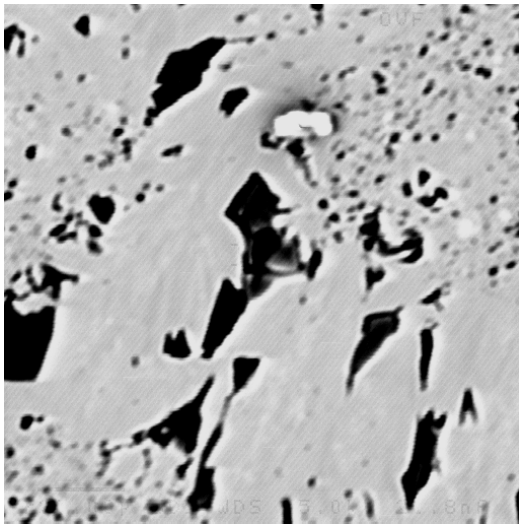
e.



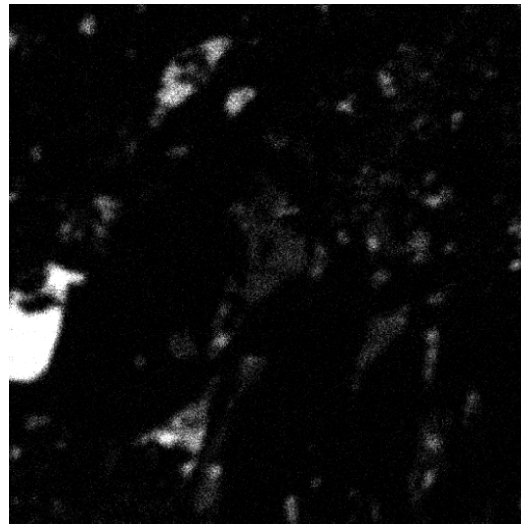
f.

Figure 3. Electron microprobe and SEM images of scale from the Elmore-12 well. Figures 3a-3d illustrate the fibrous texture and general composition of iron-rich smectite from the microprobe analyses (ABS = absorbed image; see Table 2 for the quantitative chemistry). Figures 3e and 3f show a SEM image and corresponding EDX spectra of dense, conchoidally-fractured amorphous iron silicate in the scale.

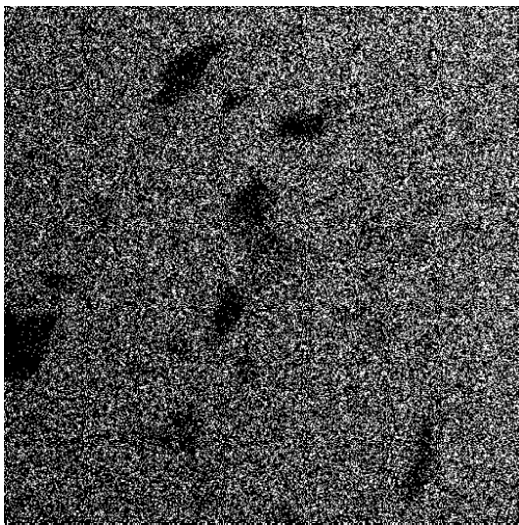
SJL01003



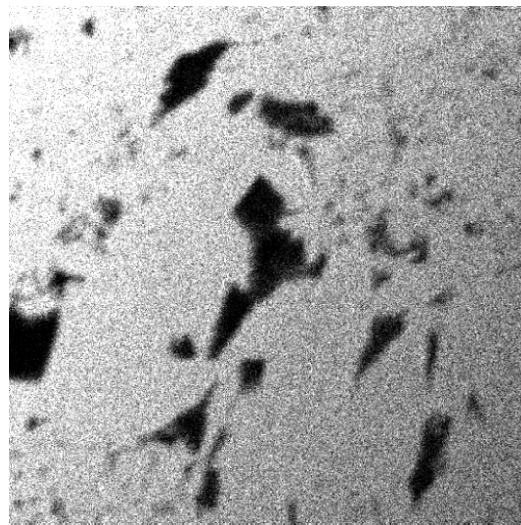
a. ABS



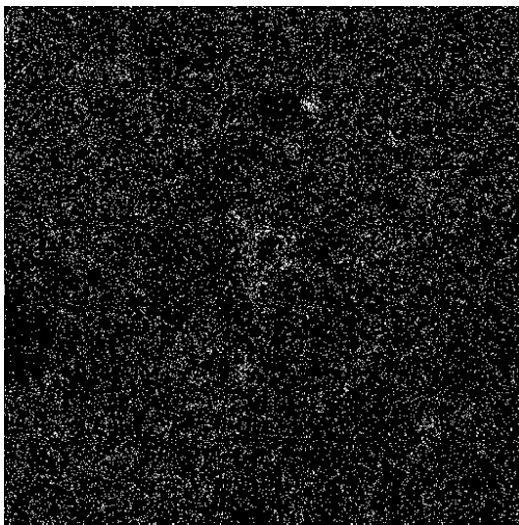
b. Ca



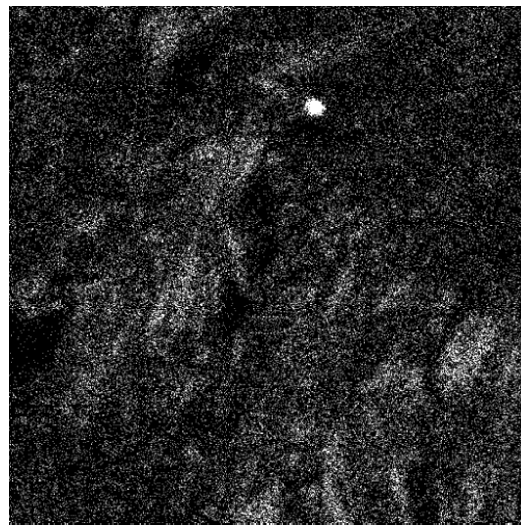
c. Fe



d. As



e. Cu



f. S

40010715

*Figure 4. Electron microprobe imagery and element mapping of scale from the River Ranch 18 well. The backscattered electron image (Fig. 4a; ABS = absorbed) shows the bladed character of coarsely-crystalline loellingite. The element maps illustrate the occurrence of calcite (see Ca in Fig. 4b) and chalcopyrite (Cu and S in Figs. 4e and 4f) in the interstitial areas between loellingite crystals (Fe and As in Figs 4c and 4d).*

**Table 1. Whole-Rock and Trace Element Analyses of Production Well Scales from the Salton Sea Geothermal Field**

Sample	SI-10 <sup>1</sup>	SI-11 <sup>1</sup>	EL-12 <sup>2</sup>	RR-18 <sup>2</sup>	Sample	SI-10 <sup>1</sup>	SI-11 <sup>1</sup>	EL-12 <sup>2</sup>	RR-18 <sup>2</sup>
Oxides (wt %)					Trace Elements (ppm)				
SiO <sub>2</sub>	38.45	28.40	37.95	1.16	Cu	105	321	30	8280
TiO <sub>2</sub>	0.02	0.03	<0.01	<0.01	Pb	517	880	bdl	45
Al <sub>2</sub> O <sub>3</sub>	3.29	2.59	3.08	0.26	Zn	691	20866	320	20
Fe <sub>2</sub> O <sub>3</sub> *	34.43	32.67	30.53	35.64	Ag	5	7	3	33
MnO	0.69	0.59	0.33	0.03	As	77	237	140	<b>65.4%</b>
MgO	3.19	2.57	6.15	0.09	Au	0.108	0.096	0.385	<b>233.0g/t</b>
CaO	1.38	1.34	0.85	3.82	Bi	14	18	bdl	9660
Na <sub>2</sub> O	0.76	1.83	2.28	0.56	Co	6	10	35	2420
K <sub>2</sub> O	0.39	0.61	0.96	0.22	Cr	21	57	bdl	bdl
P <sub>2</sub> O <sub>5</sub>	0.22	0.07	<0.01	0.09	Li	22	47	na	na
LOI	na	na	12.93	39.84	Mo	2	16	bdl	35
sum	82.82	70.69	95.06	81.71	Ni	22	23	85	370
Cl (ppm)	na	na	16000	5460	Sb	61	52	60	3600
S (%)	0.10	0.39	0.03	0.92	W	bdl	5	bdl	bdl
					Ba	501	461	40	bdl
					Cs	11.3	12.2	23.3	1.3
					Ga	36	29	53	bdl
					Gd	0.6	0.6	bdl	0.3
					Rb	29	38	73	9
					Sr	147	156	94	72
					V	186	198	80	bdl
					Y	10	7	bdl	5

Samples were analyzed by a combination of AA, ICP-AES and ICP-MS (inductively coupled argon plasma optical emission spectrometry) techniques by <sup>1</sup>Activation Laboratories Ltd. of Toronto, Canada, and <sup>2</sup>ALS Chemex Labs of Sparks, Nevada. Sulfur was analyzed by a LECO-IR Detector. Chlorine was analyzed by NAA. The gold as g/t was analyzed by a FA-gravimetric method.

\*All iron reported as Fe<sub>2</sub>O<sub>3</sub>. Abbreviations: na = not analyzed, bdl = below detection limit.

**Table 2. Microprobe Analyses of Nontronite Clay Scale Sample from Well Elmore-12**

sample	EL-12a	EL-12b	EL-12c
Oxides (wt %)			
SiO <sub>2</sub>	43.53829	44.35225	43.28339
TiO <sub>2</sub>	0	0.060048	0.005004
Al <sub>2</sub> O <sub>3</sub>	3.543764	3.522985	3.339752
Fe <sub>2</sub> O <sub>3</sub> *	36.05641	35.83965	33.92596
MnO	0.001291	0	0
MgO	4.296561	4.266339	4.639077
CaO	0.705096	0.706495	0.664525
Na <sub>2</sub> O	1.183544	0.798016	1.201068
K <sub>2</sub> O	1.15439	1.19777	1.088115
ZnO	0.080925	0.133215	0
Sum	90.56027	90.87677	88.14690
Cl	0.484	0.558	0.37

\*All iron reported as Fe<sub>2</sub>O<sub>3</sub>.

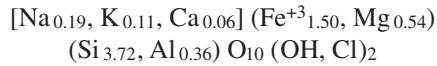
**Table 3. Microprobe Analyses of Loellingite — Scale Sample from Well River Ranch-18**

sample (wt %)	1a	1b	1c	1d	1e	1f	1g	1h	1i	1j
As	70.197	69.459	69.546	69.218	69.578	69.534	69.57	68.777	69.794	69.451
Fe	26.509	28.73	28.255	28.427	27.122	28.079	27.91	28.197	27.509	27.079
Cu	1.584	0.754	0.597	0.603	0.971	0.645	0.824	0.434	1.127	1.095
Bi	0.369	0.787	0.496	0.562	0.615	0.794	0.803	0.538	0.628	1.038
Sb	0.313	0.698	0.454	0.639	0.375	0.523	0.675	0.533	0.61	0.509
Ba	0	0.056	0	0	0.169	0	0.202	0	0.101	0.169
Ag	0.022	0	0.03	0	0.032	0	0	0	0.037	0.082
Au	0	0	0.177	0.177	0.216	0	0.207	0.029	0	0
total	98.994	100.484	99.555	99.626	99.078	99.575	100.191	98.508	99.806	99.423

sample (wt %)	2a	2b	2c	2d	2e	2f	2g	2h	2i	2j
As	69.465	68.488	70.077	69.825	69.146	70.505	68.045	22.655	36.066	44.494
Fe	28.199	28.557	27.299	27.058	29.089	26.664	27.844	19.895	15.431	22.712
Cu	0.63	0.224	1.299	1.344	0.467	1.416	0.571	6.401	2.028	3.295
Bi	0.326	0.066	0.431	0.808	0.51	0.412	0.994	0	0	0.206
Sb	0.665	0.629	0.431	0.392	0.448	0.352	0.817	0	0.032	0.326
Ba	0	0.011	0	0	0.157	0	0.09	0	0.022	0.079
Ag	0.009	0.02	0	0.045	0	0.009	0.06	0.022	0	0.009
Au	0	0	0.108	0	0	0.03	0.029	0	0.01	0
total	99.294	97.995	99.645	99.472	99.817	99.388	98.45	48.973	53.589	71.121



microprobe data shown in Table 2, a structural formula for the clay can be calculated as:



With ferric iron as the dominant cation in the octahedral site, this formula corresponds to a dioctahedral clay, close to a  $\text{Fe}^{+3}$  end-member nontronite in composition (Dana's New Mineralogy, 1997). However, other microprobe analyses indicate even more Fe in the octahedral site, suggesting that the clay has a more trioctahedral character. This, and the presence of the 060 peak near 1.53Å on X-ray diffractograms, indicates that although the clay is dominantly a dioctahedral smectite, some trioctahedral smectite (iron-rich saponite) may also be present.

The major element chemistry (Table 1) of the bulk scale sample indicates 38 wt %  $\text{SiO}_2$ , 31 wt %  $\text{Fe}_2\text{O}_3$ , 6 wt %  $\text{MgO}$ , 2 wt %  $\text{Na}_2\text{O}$ , and LOI (loss on ignition) of 13 wt % (for a total of 95 wt %). Trace element analyses yield 40 to 100 ppm Ba, Sr, Rb, and V; 30 to 85 ppm Co, Cu, and Ni; 53 ppm Ga; 23 ppm Cs; and 2410 ppm and 320 ppm of Mn and Zn, respectively. Comparison of the chemistry of the bulk sample (Table 1) with the chemistry of the clay (Table 2) suggests that most of the Zn and Mg is in the clay, whereas most of the Mn is probably in the amorphous iron silicate material.

### **Scale from Well River Ranch 18**

The River Ranch 18 well (RR-18) is a carbon-steel cased well that produces fluids with about 26 wt % TDS. The scale sample was collected from the cement hangdown liner early in 2000. The sample is a light to dark gray, botryoidally banded, mostly metallic scale with elongate prismatic crystals forming convex-outward, radiating bundles and sheaves.

Sample RR-18 consists of three major bands of scale material. The inner band (concave-inward) is sieve-textured and contains subequal amounts of loellingite ( $\text{FeAs}_2$ ) and a combination of clastic debris, carbonate and minor smectite. The arsenide occurs in rosettes of prismatic crystals that form a loose, loellingite network. Angular spaces between the crystals are partially filled with calcite. The central band has a botryoidal "cauliflower" appearance with bronzy metallic masses filling cracks between the radiating heads of loellingite crystals. The outer band consists of both microcrystalline and coarsely crystalline loellingite. Holes in the loellingite are filled with late-stage calcite.

XRD analysis suggests that two compositional varieties of loellingite may be present in the scale,

and confirms that the carbonate phase is calcite. Traces of chalcopryrite and elemental Bi are also tentatively identified by XRD. The chemistry in Table 1 shows almost a weight percent each of Bi and Cu, and electron microprobe element mapping shows small crystals containing Cu, Fe and S, which we interpret as chalcopryrite between the blades of loellingite (see Fig. 4).

The bulk chemistry of the scale, with 23.4 wt % Fe and 65.4 wt % As, indicates the dominance of loellingite (Table 1). Trace element contents include 9660 ppm Bi, 8280 ppm Cu, 2420 ppm Co, 370 ppm Ni, 230 ppm Mn, 45 ppm Pb, 35 ppm Mo, 20 ppm Zn, and 23 ppm W. The precious metal content of this scale is high with 33 ppm Ag, and 233 g/t Au (as measured by a FA-gravimetric method) which is equivalent to about 8.2 oz/tonne of Au.

Microprobe analyses (Table 3, Sample 1) indicate that much of the Cu, Ba, and Bi, and most of the Ag, Au, and Sb, is bound up in the loellingite crystal structure. Samples 2a to 2h (Table 3) represent microprobe analyses taken along a transect from the outer band of coarse-grained loellingite crystals (2a to 2g) inward toward the middle band (samples 2h to 2j). The middle band contains both loellingite and other clays or carbonate minerals (As, Fe, Cu, Bi, Sb, Ba, Ag and Au only sum from 49 to 71 wt %). Up to 6.4 wt % Cu in the middle band (analysis of sample 2h) likely indicates the presence of chalcopryrite that imparts a brassy color to the scale.

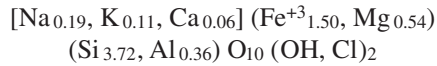
## **DISCUSSION**

### **Iron and Fe-rich Clays**

The chemistry and mineralogy of the production scales that formed in the borehole environment provide an important indication of the scales that may form within the surficial power and mineral recovery facilities. Preliminary study of deposits within reactor vessels in the power plant indicates that many of the same minerals do form there. The "gangue" minerals, calcite, barite, and fluorite, have been identified in the byproduct silica-rich filter cake from the plant. Chips of metallic material in filter cake samples are composed of iron sulfides (pyrite, chalcopryrite) and iron arsenide (loellingite), as well as Cu-Ag arsenide (domeykite and related minerals, similar to the "Line Mine" deposits described by Gallup et al., 1995). However, in contrast to the wellbore scales where poorly crystalline nontronite dominates the scale mineralogy, most of the iron silicate in the surface facilities appears to be composed of amorphous hisingerite ( $\text{Fe}(\text{OH})_3 \cdot \text{SiO}_2$ ; Gallup and Reiff, 1991).

Gallup and Reiff (1991) used Iron-57 Mossbauer spectroscopy to characterize the amorphous

microprobe data shown in Table 2, a structural formula for the clay can be calculated as:



With ferric iron as the dominant cation in the octahedral site, this formula corresponds to a dioctahedral clay, close to a  $\text{Fe}^{+3}$  end-member nontronite in composition (Dana's New Mineralogy, 1997). However, other microprobe analyses indicate even more Fe in the octahedral site, suggesting that the clay has a more trioctahedral character. This, and the presence of the 060 peak near 1.53Å on X-ray diffractograms, indicates that although the clay is dominantly a dioctahedral smectite, some trioctahedral smectite (iron-rich saponite) may also be present.

The major element chemistry (Table 1) of the bulk scale sample indicates 38 wt %  $\text{SiO}_2$ , 31 wt %  $\text{Fe}_2\text{O}_3$ , 6 wt %  $\text{MgO}$ , 2 wt %  $\text{Na}_2\text{O}$ , and LOI (loss on ignition) of 13 wt % (for a total of 95 wt %). Trace element analyses yield 40 to 100 ppm Ba, Sr, Rb, and V; 30 to 85 ppm Co, Cu, and Ni; 53 ppm Ga; 23 ppm Cs; and 2410 ppm and 320 ppm of Mn and Zn, respectively. Comparison of the chemistry of the bulk sample (Table 1) with the chemistry of the clay (Table 2) suggests that most of the Zn and Mg is in the clay, whereas most of the Mn is probably in the amorphous iron silicate material.

### **Scale from Well River Ranch 18**

The River Ranch 18 well (RR-18) is a carbon-steel cased well that produces fluids with about 26 wt % TDS. The scale sample was collected from the cement hangdown liner early in 2000. The sample is a light to dark gray, botryoidally banded, mostly metallic scale with elongate prismatic crystals forming convex-outward, radiating bundles and sheaves.

Sample RR-18 consists of three major bands of scale material. The inner band (concave-inward) is sieve-textured and contains subequal amounts of loellingite ( $\text{FeAs}_2$ ) and a combination of clastic debris, carbonate and minor smectite. The arsenide occurs in rosettes of prismatic crystals that form a loose, loellingite network. Angular spaces between the crystals are partially filled with calcite. The central band has a botryoidal "cauliflower" appearance with bronzy metallic masses filling cracks between the radiating heads of loellingite crystals. The outer band consists of both microcrystalline and coarsely crystalline loellingite. Holes in the loellingite are filled with late-stage calcite.

XRD analysis suggests that two compositional varieties of loellingite may be present in the scale,

and confirms that the carbonate phase is calcite. Traces of chalcopryrite and elemental Bi are also tentatively identified by XRD. The chemistry in Table 1 shows almost a weight percent each of Bi and Cu, and electron microprobe element mapping shows small crystals containing Cu, Fe and S, which we interpret as chalcopryrite between the blades of loellingite (see Fig. 4).

The bulk chemistry of the scale, with 23.4 wt % Fe and 65.4 wt % As, indicates the dominance of loellingite (Table 1). Trace element contents include 9660 ppm Bi, 8280 ppm Cu, 2420 ppm Co, 370 ppm Ni, 230 ppm Mn, 45 ppm Pb, 35 ppm Mo, 20 ppm Zn, and 23 ppm W. The precious metal content of this scale is high with 33 ppm Ag, and 233 g/t Au (as measured by a FA-gravimetric method) which is equivalent to about 8.2 oz/tonne of Au.

Microprobe analyses (Table 3, Sample 1) indicate that much of the Cu, Ba, and Bi, and most of the Ag, Au, and Sb, is bound up in the loellingite crystal structure. Samples 2a to 2h (Table 3) represent microprobe analyses taken along a transect from the outer band of coarse-grained loellingite crystals (2a to 2g) inward toward the middle band (samples 2h to 2j). The middle band contains both loellingite and other clays or carbonate minerals (As, Fe, Cu, Bi, Sb, Ba, Ag and Au only sum from 49 to 71 wt %). Up to 6.4 wt % Cu in the middle band (analysis of sample 2h) likely indicates the presence of chalcopryrite that imparts a brassy color to the scale.

## **DISCUSSION**

### **Iron and Fe-rich Clays**

The chemistry and mineralogy of the production scales that formed in the borehole environment provide an important indication of the scales that may form within the surficial power and mineral recovery facilities. Preliminary study of deposits within reactor vessels in the power plant indicates that many of the same minerals do form there. The "gangue" minerals, calcite, barite, and fluorite, have been identified in the byproduct silica-rich filter cake from the plant. Chips of metallic material in filter cake samples are composed of iron sulfides (pyrite, chalcopryrite) and iron arsenide (loellingite), as well as Cu-Ag arsenide (domeykite and related minerals, similar to the "Line Mine" deposits described by Gallup et al., 1995). However, in contrast to the wellbore scales where poorly crystalline nontronite dominates the scale mineralogy, most of the iron silicate in the surface facilities appears to be composed of amorphous hisingerite ( $\text{Fe}(\text{OH})_3 \cdot \text{SiO}_2$ ; Gallup and Reiff, 1991).

Gallup and Reiff (1991) used Iron-57 Mossbauer spectroscopy to characterize the amorphous

silicate scale. They found that high-temperature scales from Salton Sea production wells contained iron bound to silica with iron present in the ferric (+3) oxidation state, while the iron in iron-rich silica sludge deposited from low-temperature brine in the surface facilities consisted of subequal amounts of ferric and ferrous iron in the silicate structure. This study indicates that the smectitic clay deposited in the Sinclair and Elmore production well scales contains predominantly ferric (+3) iron in octahedral coordination, forming a dominantly dioctahedral smectite (i.e., nontronite). Thus, this study also shows that the high temperature wellbore environment favors ferric iron bonding with the silica.

This is the first description of the presence of a crystalline iron-rich clay in the scale samples rather than amorphous iron silicate. X-ray diffraction analyses of the Sinclair and Elmore well scales clearly identify the presence of a smectite clay with a basal spacing of 14 to 15 angstroms which swells to 17 angstroms upon glycolation of the sample. In thin-section analysis, the birefringence of the fibrous clay under crossed nichols indicates that it is indeed a fine-grained, crystalline compound. Electron microprobe and SEM-EDX analyses indicate that the composition of the nontronite is similar to the glassy iron silicate but differs in containing slightly more Mg and less Mn than the glass. Finally, back-scattered electron images from both the microprobe and the SEM illustrate perhaps the most important difference between these two compounds, their texture. The iron silicate is a dense, banded glass that tenaciously adheres to the well casing, and the clay is fibrous and porous. This may be the key to differences in the behavior of scales from different wells that appear to have similar chemical compositions. Apparently, the dense iron silicate glass in the Elmore well scales is extremely difficult to remove even in non-ferrous, titanium-cased wells, and the soft, fibrous clay in the Sinclair wells is much easier to clean out using mechanical means (T. Van de Putte, personal communication).

### Precious Metals

McKibben et al. (1990) discuss the chemistry and mineralogy of Au-bearing arsenide scales from Salton Sea wells that appear to be similar to our study scale from Well RR-18. They described loellingite-rich scales formed at the flashpoint in some wells with up to 40 wt % As, 2 wt % Bi, 1 wt % U, and 0.1 wt % Au. McKibben and Hardie (1997) emphasized that Au concentrations in the brine are at the ppb level (at most up to 2 ppb), and suggested that Au in the brines is transported as complexes (Au-HS<sup>-</sup>, and

possibly Au-As or Au-NH<sub>3</sub>) that become destabilized by gas loss during boiling.

The formation of the metallic loellingite scale rather than iron silicate scale may also be related to the casing material. In well RR-18, the carbon steel casing is lined with cement. Although the exact mechanisms of metal deposition are unknown, perhaps the carbon steel acts to reduce the arsenic and cause precipitation of the iron arsenide, and/or the increased surface area provided by the cement caused the metallic scale to preferentially deposit. Similar processes were evoked for the collection of precious metals from the brine in the "Line Mine" (Gallup et al., 1995).

### SUMMARY AND CONCLUSIONS

Scales from production wells in southern part of the Salton Sea geothermal field are predominantly composed of a poorly crystalline, fibrous to botryoidal, iron-rich smectitic clay of nontronite composition. X-ray diffraction results and calculations of mineral formulas based on electron microprobe data suggest that the smectite is dominantly dioctahedral in structure. Minor amounts of magnetite, Ca-Fe-Mn carbonates, and sphalerite are also present. Scales dominated by soft nontronite clay are much more amenable to periodic wellbore cleanout than are glassier and harder varieties consisting mostly of amorphous iron silicate.

Comparison of the scale chemistry from titanium-cased wells indicates that there is a relationship between the brine chemistry in different production areas and the composition of the scales. Compared to the southern part of the geothermal field, production brines in the northeast are more saline, and production well scales are more metallic, containing 20 to 90 wt % loellingite (FeAs<sub>2</sub>). Microprobe analyses indicate that some of the Cu, Ba, and Bi, and most of the Ag, Au, and Sb, is bound up in the loellingite crystal structure. Trace element chemistry indicates almost a weight percent each of Cu and Bi, and the equivalent of 8 ounces per tonne of Au in some metallic scale samples.

Acknowledgements- We'd like to thank the management of CalEnergy Operating Corp. for permission to publish this paper, as well as former employees of CalEnergy; Alex Schriener, Jr., Mark Walters and Melinda Wright, for their help during the initial stages of this project. Funding for SJL and JBH was conducted under DOE/Geothermal Grant Number DE-FG07-00ID13891.

## **REFERENCES**

- Featherstone, J., Butler, S., and Bonham, E., 1995, Comparison of crystallizer reactor clarifier and pH mod process technologies used at the Salton Sea geothermal field: Proceedings of the World Geothermal Congress, Florence Italy, v. 4, p. 2391-2394.
- Gaines, R.V., Skinner, H.C.W., Foord, E.E., Mason, B., Rosenzweig, V.T., and King, V.T., 1997, Dana's New Mineralogy, Eighth Edition: John Wiley & Sons, New York, 1819p.
- Gallup, D.L., 1989, Iron silicate scale formation and inhibition at the Salton Sea geothermal field, *Geothermics*, v. 18, p. 97-103.
- Gallup, D.L., and W.M. Reiff, 1991, Characterization of geothermal scale deposits by <sup>57</sup>Fe Mossbauer spectroscopy and complementary X-ray diffraction and infra-red studies: *Geothermics*, v. 20, p. 207-224.
- Gallup, D.L., Featherstone, J.L., Reverente, J.P., and Messer, P.H., 1995, Line Mine: A process for mitigating injection well damage at the Salton Sea, California (USA) geothermal field: Proceedings of the World Geothermal Congress, Florence Italy, v. 4, p. 2403-2408.
- Geothermal Resources Council, 1999, CalEnergy signs zinc sales agreement: U.S. Industry News, GRC Bulletin, September/October 1999, p. 201.
- McKibben, M.A., Williams, A.E., and G.E.M. Hall, 1990, Solubility and transport of platinum-group elements and Au in saline hydrothermal fluids: constraints from geothermal brine data: *Econ. Geol.*, v. 85, p. 1926-1934.
- McKibben, M.A. and Hardie, L.A., 1997, Ore-forming brines in active continental rifts: Chapter 17 in, H.L. Barnes, ed., *Geochemistry of Hydrothermal Ore Deposits*, Third Edition, p. 877-927.
- Moore, D.M. and Reynolds, R.C. Jr., 1989, *X-ray Diffraction and the Identification and Analysis of Clay Minerals*: Oxford University Press, New York, 332p.
- U.S. Department of Energy, 1999, Coproduction, producing even cleaner power: *Geothermal Today*, 1999 Geothermal Energy Program Highlights, p. 22-25.